International Research Journal of Multidisciplinary Scope (IRJMS), 2025; 6(3):1575-1586

Original Article | ISSN (O): 2582-631X DOI: 10.47857/irjms.2025.v06i03.04563

Development and Classification of L-Asparagine, Metal Compound Amino Acid NLO Semiorganic Crystals

S Silambarasan*, R Vadamalar, P Prveena, A Arun Raj

Department of Physics, Muthurangam Govt College affiliated by thiruvalluvar university, vellore, tamilnadu, India. *Corresponding Author's Email: ssilambarasan7658@gmail.com

Abstract

L-asparagine potassium nitrate was prepared and crystallized in the form of a single crystal by the slow evaporation solution growth method. The obtained crystal was colourless, brilliant, and transparent with well-defined facets, which suggested high purity. Synthesis was performed in a 1:1 molar ratio of L-asparagine and potassium nitrate, and the process of crystal growth was monitored carefully for 15 days. Elemental analysis revealed the anticipated stoichiometric composition of the compound. X-ray diffraction analysis showed sharp, well-defined Bragg peaks, establishing the crystalline nature of the material and determining it to have an orthorhombic crystal system. The optical behavior of the crystal was investigated using UV–visible (UV-vis) spectroscopy, which revealed good transparency in the visible range with a cutoff wavelength of approximately 250 nm, indicating its suitability for optical applications. The bandgap energy was calculated to be 4.7 eV. Fourier transform infrared (FTIR) spectroscopy was employed to determine different functional groups, with characteristic absorption bands representing O-H, N-H, and C=O stretching vibrations, establishing the molecular structure. The Non-Linear Optical (NLO) characteristics of the synthesized compound were studied by the Kurtz and Perry powder method, which indicated that the Second-Harmonic Generation (SHG) efficiency of the compound was 0.68 times greater than that of potassium dihydrogen phosphate (KDP), a reference NLO material. These results indicate that L-asparagine potassium nitrate is a good candidate for optoelectronic and photonic device applications.

Keywords: Elemental Analyses, Optical Properties, Potassium Dihydrogen Phosphate, Structural Features.

Introduction

NLO represent as nonlinear optical crystals were attracted excessive arrangement of interest since of their prospective uses in ophthalmic data processing, regularity conversion, and light sensitive storage of data disk (1). Acids of amino offer desirable tools of NLO uses because it has acid of carboxyl (COOH) and amino of Hydrogen acceptor (NH^{+2}). Related to mineral crystals, carbon-based crystals have been found to have far larger nonlinear susceptibilities, but their utility was limited by low automatic qualities and the incapability to grow enormous quartzes (2). Rapid and nonlinear reactivity was a characteristic of organic crystals. Intrinsic restrictions include things like volatility, poor current stability, and weak powered strength. Numerous plants utilize the obviously occurring amino acid as a source of nitrogen reserves and as a metabolic regulator of approximately cell activities in spirit and brain tissues (3). Two NLO materials were recently undergone the creation and characterization of single crystals (4). Using the in-formation from the previous section as a foundation; it presented the creation, spectra, and nonlinear optical description of the crystal.

A significant and sustained global effort was one of the materials of NLO used for development and synthesis purposes. Since NLO materials were the fundamental building blocks of an industrial photonic and electronic in terms of technology (5). Since single crystals were necessary for many different fields, including optoelectronics, telecommunication, optical modulation, and switching devices, etc., the fundamental building blocks of contemporary science and technology (6, 7). From this perspective, research on metal-organic crystals was particularly explored. The π-bond coordination that spans the molecule's length was the foundation of the organic crystal structure, and the substitute of electron donation and withdrawn category was quickly manipulated the aromatic moieties, which increases optical nonlinearity (8). Furthermore, the form of materials in organic crystals were inexpensive and

(Received 20th March 2025; Accepted 17th July 2025; Published 30th July 2025)

easy to fabricate devices from, they were of tremendous industrial importance. Most organic materials have good nonlinear coefficients and were manipulated and incorporated into various structures. These materials had minimum mechanical strength and less thermal behavior of primary shortcomings caused by the process of laser damage. The compound was inorganic and offered superior mechanical and thermal qualities. However, because there was no π-electron delocalization, these inorganic compounds have only minor NLO properties. Therefore, this difficulty was solved by creating a crystal at semi-organic that mix advantageous aspects of molecules at organic and inorganic to produce good NLO characteristics (9).

The recent technology of Laser, optical communication, and optical data storage was significantly impacted by the optical frequency of conversion materials in nonlinear. Over the past ten years, organic compounds have been the main focus of the quest for new frequency conversion materials (10, 11), and numerous materials of NLO organic with important factors were found in nonlinear. Nevertheless, low laser damage threshold, poor optical quality, and frequently insufficient transparency have hindered the use of applications in materials at organic and crystal at single. Because of its substantial nonlinearity, great resistance to damage caused by lasers, minimum sensitivity of angular, and good mechanical hardness, semi-organic materials had drawn the attention of researchers recently (12-14). The nonlinear ultrasonic technique known as SHG was identifying and microstructural tracking of alternative metals. The following mechanism was involved such as a second harmonic wave was produced when a sinusoidal ultrasonic wave interacted with microstructural characteristics while it was propagating through a material. The acoustic nonlinearity parameter, β, was used to quantify this impact. In recent times, there has been a notable emphasis on SHG measurement techniques in academic literature. This was attributed to the growing significance of structural component reliability and integrity in ensuring the operation at safe of structures in critical, such as the industries based on aviation, transportation, and energy (15).

In the research work, the synthesis and development of single crystal along with its physical properties' characterization of the produced semi-organic NLO crystals that were investigated using many characterization techniques. For existing publications, no systematic research has been done on this area. Characterization investigations including X-Ray Diffraction Analysis (XRD), FTIR, UV–Vis, NLO, Photoluminescence (PL), EDS, Thermogravimetric (TG) / Differential Thermal Analysis (DTA), and etching studies were part of our inquiry.

Methodology

Synthesis of Materials and Crystal Growth

Analytical-grade L-asparagine (Sigma-Aldrich, ≥99%), and potassium nitrate (Merck, AR grade) were used as received without further purification. A solution was prepared at 1:1 molar ratio where 1.32 g of L-asparagine and 1.01 g of potassium nitrate were dissolved in 50 mL (16) of double-distilled water. A magnet stirrer was used for continuous stirring at room temperature (~28 ± 2°C) for 1 hour, or until was completely homogeneous and transparent. After that, the homogeneous mixture was created by gradually adding potassium nitrate to the solution while stirring continuously. Then there was silence in return. After about 15 days, two recrystallizations were performed on potassium nitrate crystal of L-asparagine to improve their purity. The crystals were harvested and recrystallized to improve purity, as reported in past study (17).

The solution was then filtered with Whatman No. 1 filter paper and then moved into a clean glass 100 mL beaker. The beaker was capped with aerated aluminum foil permitting slow evaporation and protection from contamination. Once set, the beaker was placed in a clean area at room temperature, right measured, and exposed to ambient light. The final crystals were colourless, brilliant, and showed good faceting, as seen in Figure 1 (A) and Figure 1 (B).

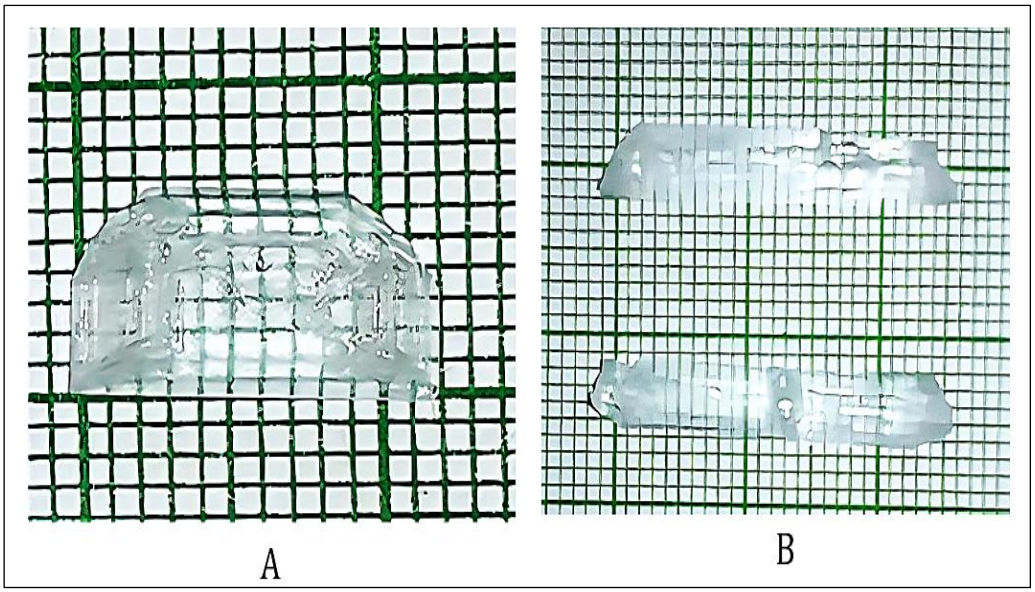

Figure 1: (A) As-Grown Single Crystal of L-Asparagine Potassium Nitrate after 15 Days (Scale Bar = 200 Mm), (B) Recrystallized Crystal Showing Enhanced Clarity and Size (Scale Bar = 200 Mm)

Fifteen days later, distinct, transparent single crystals were found at the bottom of the beaker. These crystals were carefully collected and subjected to two successive recrystallizations using the same slow evaporation method to improve crystal clarity and purity.

Characterization Analysis

XRD analysis was performed using a Rigaku SmartLab diffractometer with Cu-Kα radiation (λ = 1.5418 Å), operated at 40 kV and 30 mA. FTIR spectra were recorded using a PerkinElmer Spectrum II in the range 4000–400 cm^{-1} using KBr pellet method. UV–Vis analysis was carried out using a Cary 50 spectrophotometer in the range of 200–800 nm. FTIR was used to functional group identification. To carry out SHG utilizing in Kurtz and Perry (18), which is still popular for assessing non-centrosymmetric NLO materials. In the past, one study provided a recent examination of the Kurtz and Perry method of identifying SHG with an emphasis on reference selection and consistency of measurement (19), which continues to demonstrate the applicability of using the Kurtz and Perry method in research involving semi-organic NLO crystals. Revisited Kurtz and Perry method highlights improvements in powder grain size control, calibration standards, and reference crystal comparison, which were considered during our SHG testing. To use of luminescence spectrometer of Perkin Elmer LS45 to detect photoluminescence between 200 to 700 nm. The microscopic analysis at the etching density in various time intervals was employed for etching research.

Results and Discussion

X-Ray Diffraction Analysis (XRD)

At room temperature, XRD results were accomplished using a Rigaku X-ray diffractometer using $C_{uK\alpha}$ (1.5415) radiation. Figure 2 shows the deflection pattern of the crystal. The XRD pattern's distinct, well-defined peaks demonstrate the extraordinary crystallinity of the manufactured L-asparagine single crystal. It was charity to index the described powder X-ray deflection pattern (20). The lattice constants a = 12.895, b = 6.6023, and c = 4.645 characterize the orthorhombic structure of crystals. The different peaks were observed concerning angle. For identification of the crystal growth in terms of Bragg's angle was 18^o, 22^o, and 30^o corresponding plane [210], [201], and [310] respectively.

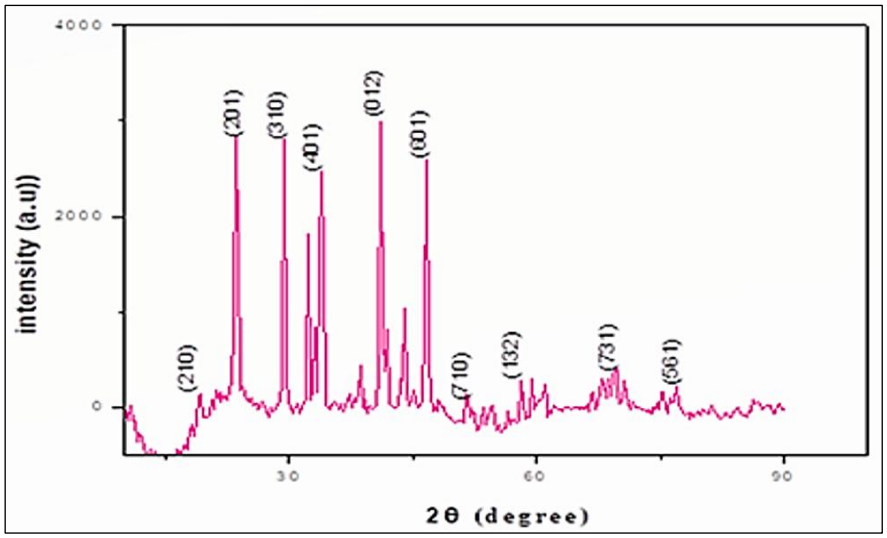

Figure 2: Powder X-ray Diffraction Pattern of LAPN Crystal

The presence of sharp and distinct diffraction peaks indicates the crystalline nature and orthorhombic structure of LAPN. Indexed peaks corresponding to major planes support the purity and phase identity of the synthesized material. For collecting the XRD data from high precision 3D axis goniometer monochromatic light source with single crystal CCD diffractometer. Diffracted intensities were collected from 3 distinct zones of crystallography, the lattice parameters were analysed (21).

Infrared Fourier Transform Spectral Study

Using Fourier transform infrared (FTIR) spectroscopy, the group of functional materials and modes of trembling from the amino crystal were identified. The FTIR spectra crystal was obtained in the range of 4000–400 cm^{-1} using a Perkin Elmer spectrometer II in imperative to qualitatively examine the manifestation of functional groups. Figure 3 displays the L-asparagine potassium nitrate FT-IR spectrum. FTIR spectra's vibration frequency assignments were shown in These correspond with the stated numbers (22). Water molecules' O-H stretching vibrations cause the 2929 cm^{-1} and 3395 cm^{-1} bands to form, whereas CO_2 molecules' symmetric stretching vibrations cause the 1560 cm^{-1} band to form. The FTIR spectrum recorded was displayed in Figure 3.

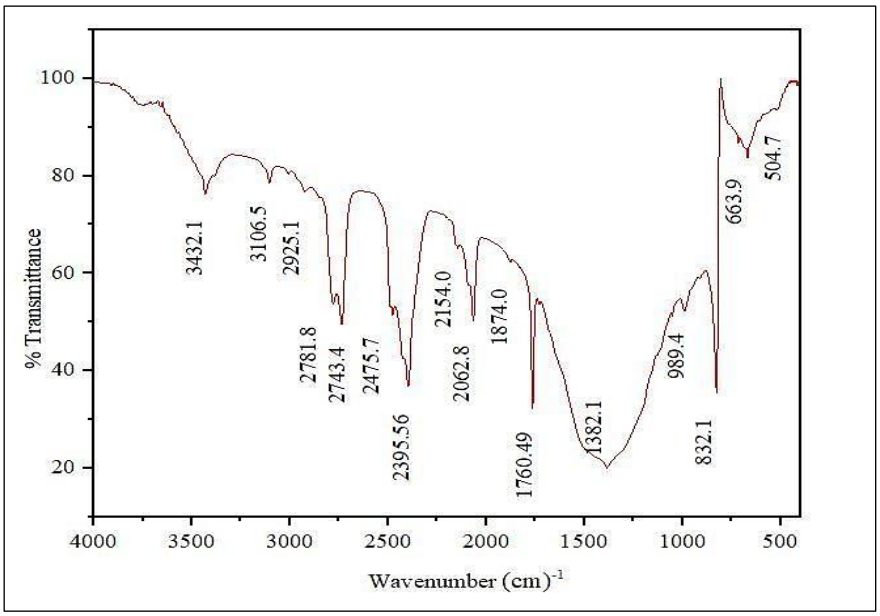

Figure 3: FTIR Spectrum of LAPN Crystal

By using FTIR measurement, different group of functional materials and type of vibrations of chemical bonding were examined. FTIR spectra were used to pellet of KBr was collected in region of 4000–400 cm^{-1}.

UV -Visible Analysis

The optical characteristics of the LAPN crystal synthesized were analysed using UV-Visible spectroscopy. The transmittance spectrum was taken between 200 and 800 nm with a Varian Cary 50 spectrometers. The crystal demonstrates very good optical transparency of over 97% in the visible region with a very sharp absorption edge near 250 nm, showing high optical quality, and indicating possible applications in optoelectronics. The transmittance spectrum taken is shown in Figure 4.

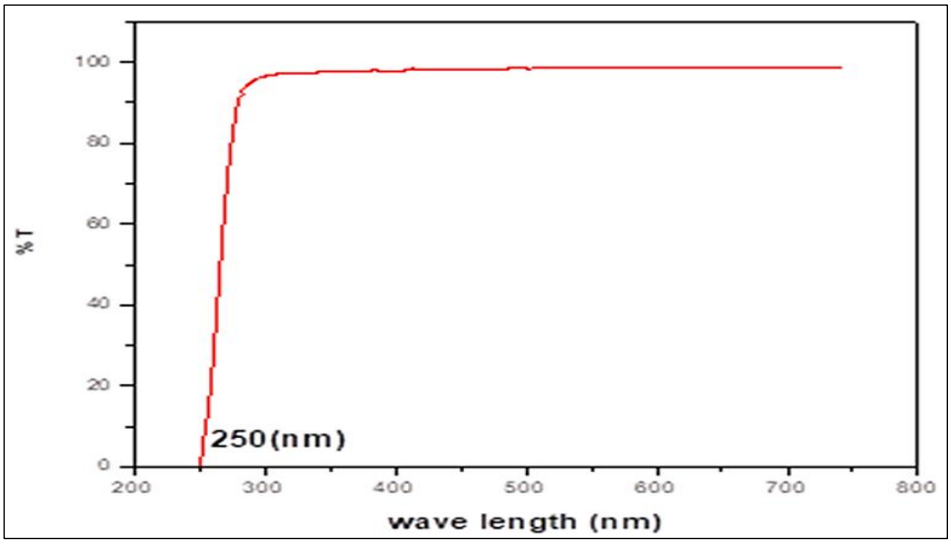

Figure 4: UV-Visible Spectrum of LPAN Crystal

The spectrum shows high transparency in the visible region and a sharp cut-off in the UV regime near 250 nm, and demonstrates optical purity suitable for NLO applications. The optical band gap (E_g) for the LAPN single crystal was calculated using the Tauc plot method. The absorption coefficient (α) was calculated from the transmittance spectrum using Equation [1], while the band gap was determined through the linear portion of the $(\alpha h\nu)^2$ vs. photon energy ($h\nu$) plot from which Equation [2] was derived. The linear region indicated by the slope was extrapolated to the energy axis, demonstrating the E_g, as illustrated in Figure 5. The estimated band gap for the single LAPN crystal studied was 4.7 eV, which is a measure of strong electronic insulation and suggests use in photonic applications (23).

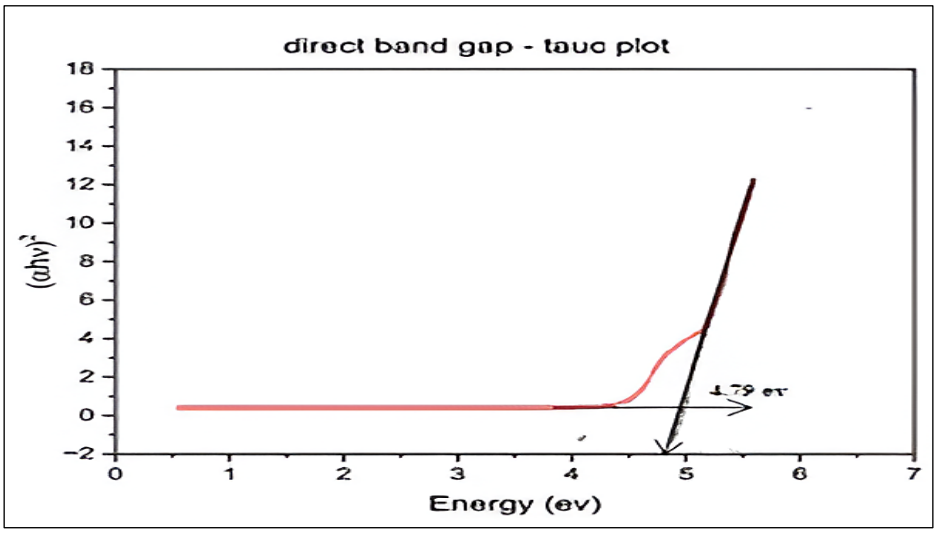

Figure 5: Tauc Plot for Band Gap Estimation of LAPN Crystal

The band gap energy was determined as 4.7 eV by extrapolating the linear region of the $(\alpha h\nu)^2$ vs $h\nu$ plot of LAPN and thereby confirming the wide-band-gap behavior typical of NLO materials.

The characterisation of structure at atomic, bandgap electronic, and electrical of materials were intimately related to their transmittance and absorption behaviours. To determine whether or whether a developed single crystal was appropriate for a certain optical application, it was crucial to ascertain these qualities (24). Figure 4 displays that the optical spectrum of transmittance measured in 200–800 nm wavelength range. The optical transparency sample has good through the entire spectrum visible. The primary absorption was discovered that line was below 280 nm. The absorbance behaviour was reduced in range of visible and supported growth of l-asparagine and the metal's suitability for NLO applications. The currently investigated chemical proves helpful in the creation of NLO devices. Moreover, the transmittance (T) spectrum was used to estimate the absorption coefficient, which plays a significant role for optical components (25).

$$\alpha = \frac{2.3026}{t} log_{10}\left(\frac{100}{T}\right) \quad [1]$$

Where T represent the transmittance sample's (%) and t were its thickness. The calculation of band gap using the following relationship:

$$(\alpha h\upsilon)^2 = A(h\upsilon - E_g) \quad [2]$$

Where h represents Planck's constant, ω represent incident beam frequency, and A represent constant. An extrapolated linear behavior was seen in the depicted curve among photon energy ($h\upsilon$) and $(\alpha h\upsilon)^2$ (26). The optical energy estimation of band gap (E_g) involves extending the segment of linear in curve to the $(\alpha h\upsilon)^2$ zero point, depicted in Figure 5. For the sample under study, the optical energy bad gap (E_g) was determined as 4.7 eV.

NLO (SHG) Measurement

Using the Kurtz and Perry approach, the Harmonic generation performance of powdered potassium nitrate L-asparagine was examined. The powdered sample was operated on a more-intensity He-ne laser at 1060 nm with pulses lasting 8 ns and 1.2 mJ of input energy per pulse (27). The SHG activity was established by the sample's vivid green fluorescence (533 nm). The LAPAN crystal produced an SHG output voltage of 4.06 mV, while standard potassium dihydrogen phosphate (KDP) produced 6.00 mV. The effectiveness of SHG is summarized in Table 1, which compares the SHG output of LAPN with that of standard KDP.

Table 1: SHG Efficiency of LAPN and KDP Crystals

Material	NLO Output	SHG Efficiency
LAPN	4.06mV	0.68 (times of KDP)
KDP	6mV	-

The above table indicates that the LAPN achieved 0.68 times the SHG efficiency of KDP. This reinforces the non-centrosymmetric nature of the LAPN crystal. The second harmonic signal was collected with a lens, and the output signal was detected with a photomultiplier tube. The result performs the LAPN can potentially be used in LED and optical switching applications. Doping with urea increases SHG efficiency because it increases the amount of charge carriers (28).

Potassium (K^+) ions are not directly involved in electronic transitions due to their closed shell (no d-electrons), but they help stabilise the crystal lattice. Transition metal ions (Cu^{2+}, Co^{2+} etc.) allow for d–d transitions that can alter the crystal field symmetry while K^+ helps keep everything uniform and leads to very high transparency in the optical region. This structural arrangement is critical for efficient second harmonic generation (SHG) and assures the non-centrosymmetry, which are the two main characteristics for materials to have nonlinear optical properties.

L-asparagine has polar functional groups in the amino group ($-NH_2$) and carboxylic acid group (–COOH) that will have a permanent dipole moment. Because of these polar groups, this crystal can

make strong interactions with light. If the molecular structure has a non-centrosymmetric crystal system (CRS), such as the orthorhombic system used in this experiment, then the molecular dipoles can align in a geometric way to enhance the nonlinear optical (NLO) effects, including second harmonic generation.

Amino acid-based ligands like L-asparagine enhance NLO activity by combining polar functional groups (–NH_2 and –COOH) with strong organizational control through hydrogen bonds. According to classical NLO theory, the second-order susceptibility (χ^2)—and thus SHG efficiency—is directly related to the first hyperpolarizability (β) of the molecule and its alignment in a non-centrosymmetric lattice. The donor (–NH_2) and acceptor (–COOH) groups create an internal push–pull system that increases β. This structural concept is supported by recent reports: for instance, amino acid-templated tin fluoride crystals demonstrate enhanced SHG (0.85 × KDP) due to polar coordination and symmetry control (29, 30). Additionally, studies on L-2-aminobutyric acid–D-methionine crystals combine experimental and quantum-chemical methods to show how dipolar amino acid ligands improve electronic transitions tied to NLO response (31). These findings align with rational structure–property design principles in modern NLO materials.

Photoluminescence Studies

The optical characteristics of crystal were investigated using PL methods. The photoluminescence spectra of potassium nitrate L-asparagine were measured among 200 and 700 nm using a Perkin Elmer LS45 luminescence spectrometer (32). The excitation wavelength used was 210 nm. A noticeable emission peak with a center wavelength of 343 nm was seen in the spectrum as depicted in Figure 6.

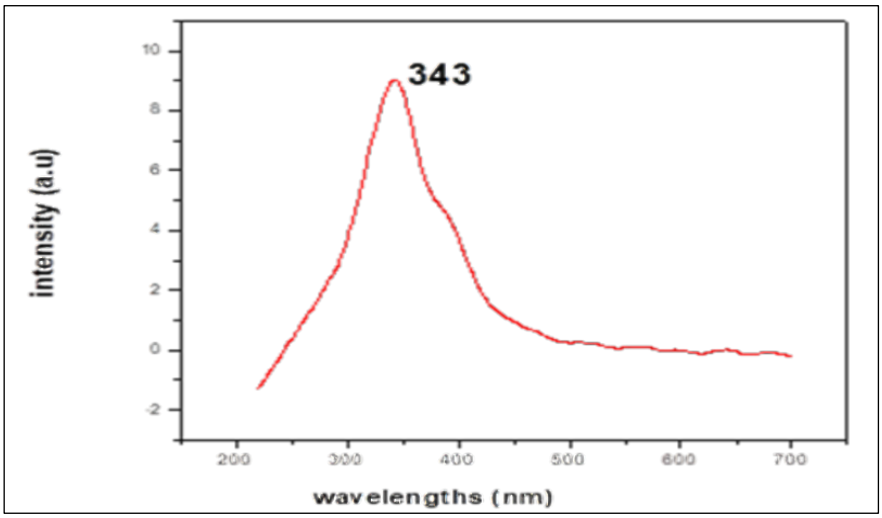

Figure 6: Photoluminescence of LPAN

Figure 6 displays the emission spectrum that was acquired between 200 and 700 nm in order to examine the formed crystal's electrical structure. The yellow emission of material was the excitation at 680 nm, as evidenced by spectra, which showed that the emission peak at broad from 450 to 700 nm and peak at sharp of 343 nm. There was peak at sharp was 620 nm in this broad spectrum, which was caused by the CO_2 group. The emission peak of broad with lower strength was caused by l-asparagine. The peak intensity was reduced gradually from 343 nm onwards because of the bond of hydrogen in lattice of crystal. The crystal force of van der Waals caused by the aromatic ring contribution to molecular association was the source of the prominent peak seen at 343 nm (33).

Energy Dispersive X-ray Method (EDAX)

EDAX was conducted to identify the elemental composition of the LAPN crystal. EDAX was a helpful tool for determining the chemical makeup of these components (34). An FGI Quanta FGG 450 SEM instrument was utilized in conducting this analysis. From the EDAX spectrum seen in Figure 7, the presence of oxygen (O), nitrogen (N), carbon (C), and potassium (K) elements are present, which is consistent with the respective chemical structure of potassium nitrate L-asparagine.

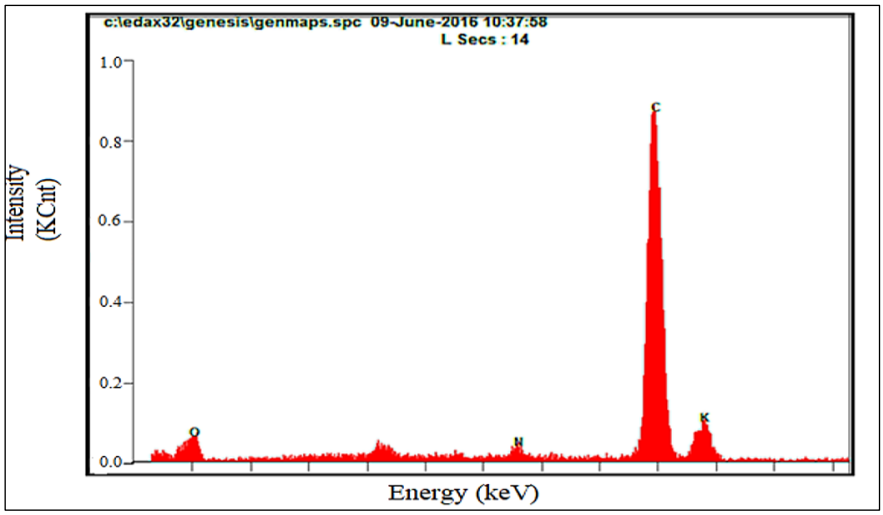

Figure 7: Energy Dispersive X-ray Analysis

The elemental peaks confirm the presence of O, N, C, and K in the synthesized crystal, validating the incorporation of L-asparagine and potassium nitrate components.

Thermal Studies (TG/DTA)

The thermal spectra of crystal were captured using a PETSZCH SPA 680C thermal analyses. The sample was frenzied in atmosphere of nitrogen among 30 and 800 °C at the rate of scanning was 20 K/min as shown in Figure 8. It displays the thermogram for semi organic crystal TG-DTA. The chemical was thermally constant up to 265 °C, according to this. As the material matures, there were three phase transitions. At 265 °C, the first phase change occurs, leading to a 4% reduction in weight. Without any mass loss, the second phase shift occurs at 433 °C. The substance has melted, according to this. The 87.6% weight loss begins at 530 °C and lasts till 656 °C. During the process, weight loss was a sign that the substance was breaking down. as a result of evaporation (35).

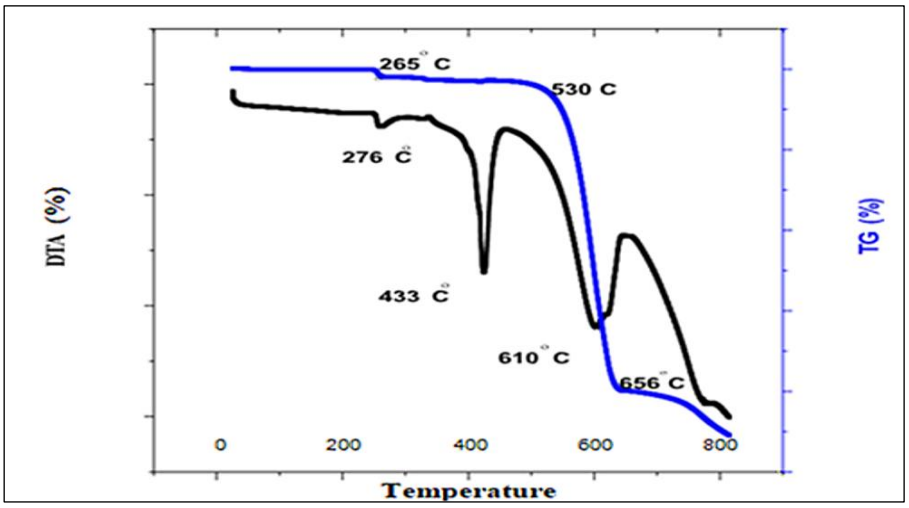

Figure 8: Thermal Analysis of LPAN Crystal

For any crystal to be used in a device, its thermal characteristics were crucial. Considerable heat was produced when cutting or treating materials with a laser. Therefore, it was crucial to look at the crystal's thermal behavior. Using a Perkin-Elmer Diamond analyzer, real-time thermogravimetric (TG) data of l-asparagine metal crystal was acquired in nitrogen environment, starts at room temperature to 800 °C at the rate of heating was 20 K/min. Figure 8 displays the plotted measured TG and DTA data. The generated single crystals of l-asparagine metal were stable in a solid state up to 265 °C.

The thermal stability of the LAPN crystal over the range of approximately 265°C is a critical finding. A significant number of devices (lasers, Optical

sensors, and photonic circuits) generate heat when in operation and, since this crystal experiences no breakdown at this high temperature, the LAPN crystal can be safely used in these devices without the risk of damage. Therefore, LAPN is appropriate for optical applications in a real-world environment.

To evaluate the overall effectiveness of the LAPN crystal that was created, a comparison with nonlinear optical (NLO) materials. The focus of the comparison will be on the optical band gap, second harmonic generation (SHG) efficiency related to potassium dihydrogen phosphate (KDP), and thermal stability related to either decomposition temperature or laser-induced damage threshold (LIDT). The benchmarking has provided a contextual framework to evaluate the potential for LAPN in NLO research and future photonic device applications. The comparative data are shown in Table 2.

Table 2: Comparison of Recently Reported Nonlinear Optical (NLO) Materials with LAPN

Material	Band Gap (eV)	SHG Output (vs KDP)	Decomposition Temp (°C)
LAPN (Our Work)	4.7	0.68	265
$CaMg_6Ga_6Se_{16}$ (36)	2.71	~4.5×	– (High LIDT)
L-histidine (37)	~4.5	High (Damage threshold 4.65× KDP)	~260*
SnP_2S_6 (38)	~2.3	$d_{33} \approx 53$ pm/V @1550 nm	Not Reported
$Sr_2ZnSn_2OS_6$ (39)	~3.5	≥1.0× $AgGaS_2$	Not Reported

In the above table, compares the optical and thermal characteristics of LAPN with recent NLO materials. While materials like $CaMg_6Ga_6Se_{16}$ and SnP_2S_6 show stronger SHG responses, LAPN provides superior thermal stability and a wide band gap suitable for visible-light optical applications. The combination of transparency and stability makes LAPN a competitive semi-organic NLO candidate.

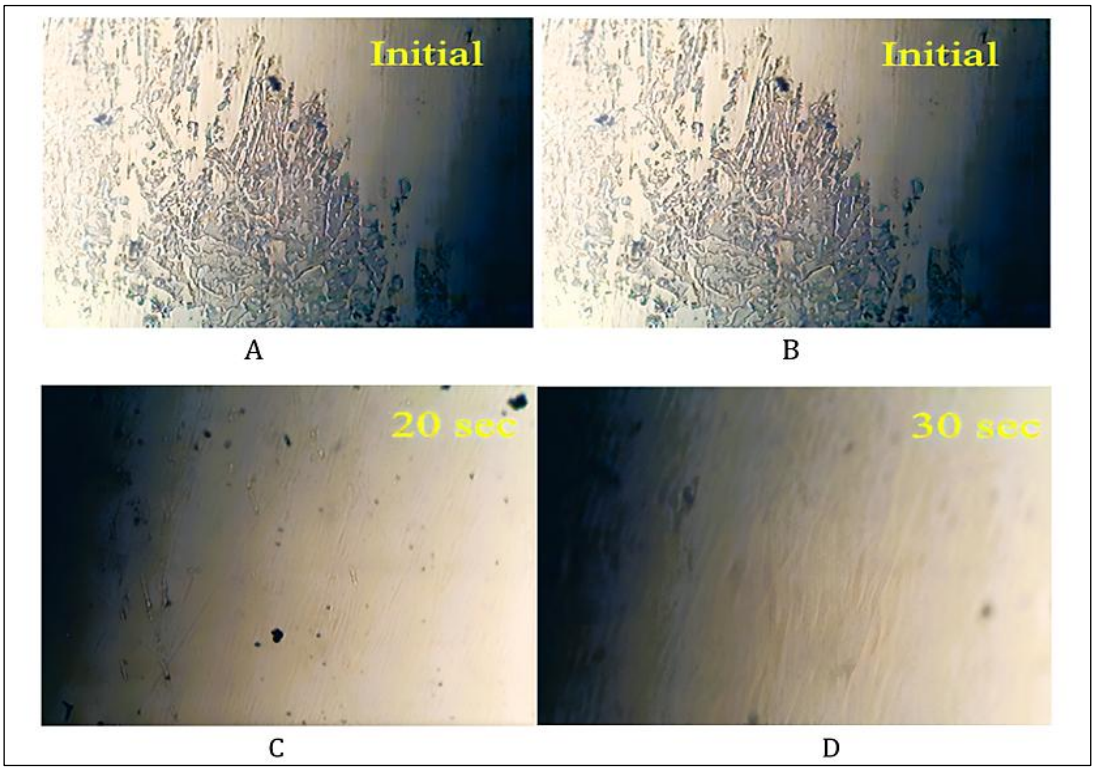

Figure 9: (A) As-Grown Crystal Surface under Optical Microscope (Scale Bar = 200 Mm), (B) Surface Etched for 10 Seconds Showing Initial Dislocation Pattern (Scale Bar = 200 Mm), (C) Surface Etched for 20 Seconds with Visible Dislocation Pits (Scale Bar = 200 Mm), (D) Surface Etched for 30 Seconds Showing Deeper Etch Pits and Uniformity (Scale Bar = 200 Mm)

Etching Studies

The dislocations in the single crystal have an impact on its quality. The dislocation disrupted the optical beam during laser processing. Therefore, growing defect-free single crystals was currently receiving a lot of research attention in an effort to create high-performance NLO devices. A straightforward method for analyzing the dislocation density using an optical microscope was chemical etching analysis. After selecting the high-quality l-asparagine metal single crystal, it was immersed in water of millipore to perform as etchant. The rectangular etching was achieved using etching times of 10, 20, and 30 seconds. Figures 9(A-D) shows that the crystal growth of l-asparagine metal surface and the same surface as etched respectively (Scale bar = 200 μm). There were no solvent inclusions or grain boundaries, indicating that the produced crystal confirms fewer dislocations. These crystals were more suited for optoelectronic and laser applications (40). The resulting dislocation patterns were viewed under an optical microscope and are shown in Figure 9.

Overall, the absence of grain boundaries and solvent inclusion indicates that the LAPN crystal was grown with low dislocation densities, making it useful for high-performing NLO and optoelectronic applications.

Conclusion

Chemical synthesis of crystals of was complete. At room temperature, water acts as the solvent throughout a process of gradual evaporation to produce crystals of high-quality Crystal. An analysis employing powder XRD revealed that the crystal structure was orthorhombic. Fourier transform study shows contains functional groups. According to UV-Vis tests, both quartzes were optically clear across the whole Ultraviolet -Vis range. The visual cut-off wavelength for was 247 nm. The light optical band gap energies of potassium nitrate of amine crystalline. According to SHG research, the SHG effectiveness of was 4.06 times greater than that of KDP. According to research on photoluminescence excitation, L-asparagine potassium nitrate was created when light with wavelengths of 235 nm and 247 nm was stimulated. EDAX tests reveal the presence of elements in Metals crystal. From the analysis of thermal readings shows that the materials at thermally stable at range of 265 °C.

Abbreviations

FTIR: Fourier Transform Infrared, LIDT: Laser-Induced Damage Threshold, NLO: Nonlinear Optical, SHG: Second Harmonic Generation, TGA/ DTA: Thermogravimetric Analysis/Differential Thermal Analysis, UV-Vis: Ultraviolet–Visible Spectroscopy, XRD: X-Ray Diffraction,

Acknowledgement

None.

Author Contributions

None.

Conflict of Interest

The authors declare that they have no conflict of interest.

Ethics Approval

This study does not contain any studies with human or animal subjects performed by any of the authors.

Funding

No funding was received for conducting this study.

References

1. Kakani SL. Material science. New Age International (P) Ltd., Publishers. 2004;1. https://www.academia.edu/9373187/Material_science_kakani_2004.
2. West AR. Solid state chemistry and its applications. John Wiley and Sons. 2022 May 9. https://www.wiley.com/en-us/Solid+State+Chemistry+and+its+Applications%2C+2nd+Edition-p-9781118447444
3. Gfroerer TH. Photoluminescence in analysis of surfaces and interfaces. Encycl Anal Chem. 2000;67:3810.
4. Arivuoli D. Fundamentals of nonlinear optical materials. Pramana. 2001;57:871-883.
5. Du C, Teng B, Wang Z, et al. Actively Q-switched intracavity second-harmonic generation of 1.06 μm in BiB3O6 crystal. Opt Laser Technol. 2002;34(4): 343-6.
6. Daniel DJ, Ramasamy P. Studies on the nonlinear optical single crystal: Ammonium d, l-tartrate (C4H9NO6). Mater Res Bull. 2012;47(3):708-13.
7. Zang Z, Zhang Y. Analysis of optical switching in a Yb3+-doped fiber Bragg grating by using self-phase and cross-phase modulation. Appl Opt. 2012;51(16): 3424-30.
8. Zang ZG, Zhang YJ. Low-switching power (<45 mW) optical bistability based on optical nonlinearity of ytterbium-doped fiber with a fiber Bragg grating pair. J Mod Opt. 2012;59(2):161-5.
9. Zang Z. All-optical switching in Sagnac loop mirror

containing an ytterbium-doped fiber and fiber Bragg grating. Appl Opt. 2013;52(23):5701-6.
10. Zang Z. Numerical analysis of optical bistability based on fiber Bragg grating cavity containing a high nonlinearity doped-fiber. Opt Commun. 2012; 285(5):521-6.
11. Pal T, Kar T, Bocelli G, Rigi L. Synthesis, growth, and characterization of L-arginine acetate crystal: a potential NLO material. Cryst Growth Des. 2003;3(1):13-6.
12. Daniel DJ, Ramasamy P. Studies on semi-organic nonlinear optical single crystal: lithium formate monohydrate (HCO2Li·H2O). Opt Mater. 2014; 36(5):971-6.
13. Karuppasamy P, Sivasubramani V, Pandian MS, Ramasamy P. Growth and characterization of semi-organic third order nonlinear optical (NLO) potassium 3,5-dinitrobenzoate (KDNB) single crystals. RSC Adv. 2016;6(110):109105-23.
14. Kishore Kumar T, Pandi S, Victor Antony Raj M, Maria Magdalene C, Prem Anand D. Growth, spectral, and thermal properties of organic nonlinear optical active morpholin-4-ium-hydroxybenzoate single crystal. Mater Manuf Process. 2010;25(9):978-81.
15. Matlack KH, Kim JY, Jacobs LJ, Qu J. Review of second harmonic generation measurement techniques for material state determination in metals. J Nondestruct Eval. 2015;34(1):273.
16. Rajarajan K, Joseph GP, Kumar SR, et al. Growth and optical studies of a novel organometallic complex NLO crystal: Tetrathiourea cadmium (II) tetrathiocyanato zinc (II). Mater Manuf Process. 2007;22(3):370-4.
17. Ambujam K, Selvakumar S, Joseph GP, Vetha Potheher I, Sagayaraj P. Thermal, optical, and electrical properties of gel grown ZMTC. Mater Manuf Process. 2007;22(3):351-6.
18. Kurtz SK, Perry TT. A powder technique for the evaluation of nonlinear optical materials. Journal of applied physics. 1968 Jul 1;39(8):3798-813.
19. Sun M, Wang G, Yao J. The Kurtz–Perry Powder Technique Revisited: A Study of the Effect of Reference Selection on Powder Second-Harmonic Generation Response. Molecules. 2023 Jan 22;28(3): 1116.
20. Krishnan C, Selvarajan P, Freeda TH. Growth and studies of pure and lithium bromide-doped zinc tris-thiourea sulphate (ZTS) single crystals. Mater Manuf Process. 2008;23(8):800-4.
21. Mahbouli Rhouma N, Rayes A, Mezzadri F, Calestani G, Loukil M. Crystal structure of non-centrosymmetric bis (4-methoxybenzylammonium) tetrachloridozincate. Struct Rep. 2016;72(7):1050-3.
22. Ambujam K, Thomas PC, Aruna S, Anand DP, Sagayaraj P. Study of optical, electrical, and magnetic properties of tetrakis thiourea nickel chloride single crystals. Mater Manuf Process. 2007;22(3):346-50.
23. Shitole SJ. Study of Structural, FT-IR and Nonlinear optical properties of Lithium iodate. International Journal on Cybernetics & Informatics (IJCI). 2012 December;1(6):1-6.
24. Tigau N, Ciupina V, Prodan G, Rusu GI, Gheorghies C, Vasile E. Influence of thermal annealing in air on the structural and optical properties of amorphous antimony trisulfide thin films. J Optoelectron Adv Mater. 2004;6:211.
25. Mott NF, Davis EA. Electronic processes in non-crystalline materials. OUP Oxford. 2012 Feb 2. https://global.oup.com/academic/product/electronic-processes-in-non-crystalline-materials-9780199645336?cc=in&lang=en&
26. Tauc J, Menth A. States in the gap. J Non-Cryst Solids. 1972;8:569-84.
27. Kumar RA, Vizhi RE, Vijayan N, Bhagavannarayana G, Babu DR. Growth, crystalline perfection and Z-scan studies of nonlinear optical alpha-lithium iodate single crystal. J Pure Appl Ind Phys. 2010;1(1):1-6.
28. Kulshrestha S, Shrivastava AK. Crystal growth and characterization of organic NLO materials and their application in optical devices. InAIP conference proceedings. AIP Publishing LLC. 2020 May 4;2220(1):050010.
29. Petrosyan AM, Kundaikar SA, Srinivasan BR. Comments on recently published papers reporting on "new" amino acid-based crystals in the Journal of Materials Science: Materials in Electronics. Journal of Materials Science: Materials in Electronics. 2023 Oct; 34(30):2052.
30. Jung A, Li Y, Ok KM. Chiral amino acid-templated tin fluorides tailoring nonlinear optical properties, birefringence, and photoluminescence. Dalton Transactions. 2024;53(1):105-14.
31. Balu R, Ayub AR, Panneerselvam A, Sumithra Devi M, Rajabathar JR, Al-Lohedan H, Devendrapandi G. Growth, experimental and theoretical investigation on the nonlinear optical, vibrational, and electronic properties of L-2-aminobutyric acid D-methionine crystal: a combined experimental and quantum chemical approach. Journal of Materials Science: Materials in Electronics. 2024 Apr;35(12):874.
32. Kumar RA, Vizhi RE, Vijayan N, Babu DR. Growth, optical and mechanical properties of nonlinear optical alpha-lithium iodate single crystal. Sch Res Lib. 2010;2(5):247-54.
33. Anandan P, Vetrivel S, Jayavel R, Vedhi C, Ravi G, Bhagavannarayana G. Crystal growth, structural and photoluminescence studies of L-tyrosine hydrobromide semi organic single crystal. J Phys Chem Solids. 2012;73(11):1296-301.
34. Chen X, Zhang L, Chang X, et al. LiMoO3(IO3): A new molybdenyl iodate based on WO3-type sheets with large SHG response. J Alloy Compd. 2007;428(1-2):54-8.
35. Matsumura S, Uematsu Y. Optical inhomogeneity of α-lithium iodate crystals. Mater Res Bull. 1972;7(1): 45-55.
36. Wang L, Chu D, Yang Z, Li J, Pan S. Wide band gap selenide infrared nonlinear optical materials A II Mg 6 Ga 6 Se 16 with strong SHG responses and high laser-induced damage thresholds. Chemical Science. 2024;15(17):6577-82.
37. Yadav S, Jewariya M, Kumari M, Nayak D, Vijayan N, Mondal T. Crystal growth and optical, nonlinear optical, thermal and terahertz time domain spectra of l-histidine single crystal: a potential terahertz material. ACS Applied Optical Materials. 2023 Oct 27; 1(11):1791-800.
38. He J, Lee SH, Naccarato F, Brunin G, Zu R, Wang Y, Miao L, Wang H, Alem N, Hautier G, Rignanese GM. SnP2S6: A promising infrared nonlinear optical crystal with strong nonresonant second harmonic

generation and phase-matchability. Acs Photonics. 2022 Apr 28;9(5):1724-32.
39. Cheng Y, Wu H, Yu H, Hu Z, Wang J, Wu Y. Rational design of a promising oxychalcogenide infrared nonlinear optical crystal. Chemical science. 2022;13(18):5305-10.
40. Karuppasamy P, Daniel DJ, Kim HJ, Pandian MS, Ramasamy P. Studies on semi-organic (C8H11NO)2[ZnCl4] single crystal for nonlinear optical (NLO) applications. J Cryst Growth. 2020; 535:125528.